ChemComm

Accepted Manuscript

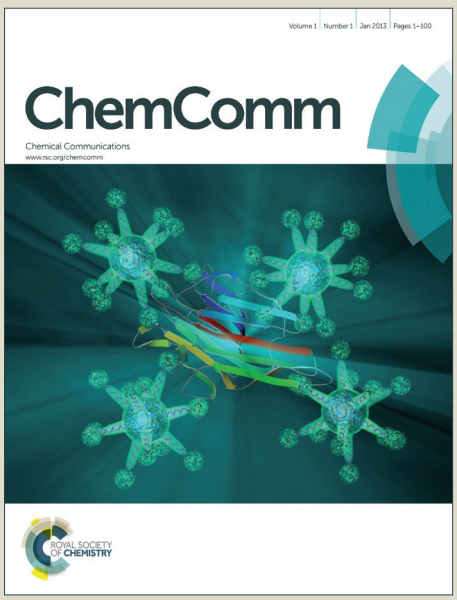

ROYAL SOCIETY OF CHEMISTRY

www.rsc.org/chemcomm

Journal Name

COMMUNICATION

A gel-ceramic multi-layer electrolyte for long-life lithium sulfur batteries

Received 00th January 20xx,
Accepted 00th January 20xx

DOI: 10.1039/x0xx00000x

www.rsc.org/

Qingsong Wang[a,b], Zhaoyin Wen*[a], Jun Jin[a], Jing Guo[a,b], Xiao Huang[a,b], Jianhua Yang[a] and Chunhua Chen[c]

A newly designed gel-ceramic multi-layer electrolyte has been used as the separator and electrolyte for lithium sulfur (Li-S) battery. The Li-S cells, free of shuttle effect, exhibit superior electrochemical performance. With almost no self-discharge, the cell demonstrates an initial discharge specific capacity of up to 725 mAh g^{-1} and remains at 700 mAh g^{-1} after 300 cycles at C/2 rate.

Rechargeable batteries with a high energy density, acceptable cycle life, and low self-discharge that go beyond the limitations of current Li-ion technology are required for the steadily increasing demands of energy storage applications, e.g., portable electronic devices, electrical vehicles and large-scale energy storage systems. Sulfur is inexpensive, nontoxic and abundant in nature, and the Li–S batteries can supply theoretical specific energy densities more than five times greater than those of Li-ion batteries. As a result, Li-S batteries are believed among the most promising next-generation electrochemical storage technologies.[1, 2].

In their conventional configuration, Li-S cells are comprised of a lithium metal anode, an organic electrolyte, and a sulfur composite cathode.[3, 4]. The cell operation starts with the lithiation of sulfur, the discharging process, and sulfur converts to Li_2S via lithium polysulfides of different chain length as intermediate species (Li_2S_x, $4 \leqslant x \leqslant 8$). The highly soluble polysulfides in the liquid electrolyte diffuse freely through the polymer separator and shuttle between the cathode and anode in the charge/discharge processes. Fundamentally, the shuttle effect becomes one of the main reasons causing Li-S batteries to have low coulombic efficiency, loss of active mass and rapid capacity fading.[5, 6] Moreover, self-discharge is also a remarkable challenge for Li-S batteries related to the soluble polysulfide species. During the cell resting, the dissolved polysulfides in the cathode side migrate to the anode side due to the concentration gradient and then directly reacts with lithium metal, resulting in a decrease in cell capacity. Apparently, all these issues are related to the liquid organic electrolyte and the porous polymer separators. The dissolution of polysulfides in liquid electrolyte is inevitable in Li-S batteries. Meanwhile, the polymer separators, serving as physically barrier between the cathode and anode, allow movements of polysulfide ions in the liquid electrolyte they absorb. In other words, the shuttle effect and capacity decay problems could be significantly suppressed but not be thoroughly avoided merely by electrode modification[4, 7-9] and electrolyte tailoring[3, 10-12].

An alternative idea to inhibit the dissolution of polysulfide species and even eliminate the shuttle effect is replacement of the conventional liquid organic electrolytes with polymer electrolytes or dense inorganic solid electrolytes.[2, 6] Solvent free solid electrolytes have been recognized as the ultimate approach to completely avoid the shuttle effect.[13, 14] However, it is critical and still a challenge to maintain good interfacial contact between the resultant solid state electrolyte and the solid electrode in Li-S batteries. A feasible way, aiming to protect Li metal in Li-air cells design, is by employing gel-polymer electrolytes (GPEs) to reduce the contact resistance where GPEs serve as buffering layer between Li metal and the solid-electrolyte membrane.[15-17] GPEs, generally consist of a polymer matrix in which liquid electrolyte is immobilized, have acceptably high room-temperature conductivities and reasonable mechanical flexibility.[18, 19] And more importantly, GPEs are able to stick to the solid electrolyte and enable the liquid electrolyte being trapped between the electrode and the solid electrolyte, helping to decrease the contact resistance of the interface. Therefore, it would be a good improvement to combine solid electrolytes with gel electrolytes to form a hybrid electrolyte to inhibit the dissolution of polysulfides and eliminate the shuttle effect. Together with novel design of cell configurations, Li-S batteries with improved cycling performance are expected to be achieved.

[a] CAS Key Laboratory of Materials for Energy Conversion, Shanghai Institute of Ceramics, Chinese Academy of Sciences, Shanghai, 200050, P.R. China.
[b] Graduate School of Chinese Academy of Sciences, Beijing, 100039, P.R. China.
[c] Department of Materials Science and Engineering, University of Science and Technology of China, Hefei 230026, P. R. China.
*Email: zywen@mail.sic.ac.cn

Electronic Supplementary Information (ESI) available: [Experimental details and additional results]. See DOI: 10.1039/x0xx00000x

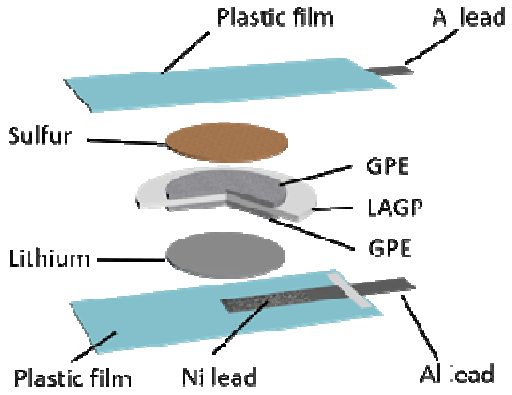

Fig. 1 Schematic illustration for the fabrication of the Li-S cell.

Here, we report a facile gel-ceramic multi-layer electrolyte (GCME), which composes of inorganic NASICON-type lithium ionic conductor $Li_{1.5}Al_{0.5}Ge_{1.5}(PO_4)_3$ (LAGP, diameter 17.5 mm and thickness 0.6 mm) and poly (ethylene oxide) (PEO)-based GPE (gel-forming liquid electrolyte 1 M LiTFSI TEGDME), for rechargeable Li-S batteries, as illustrated in Fig.1. The solvent free solid-state LAGP, which is permeable to Li-ions but impermeable to polysulfide-ions, would block the sulfur species in the cathode side and the polysulfide shuttle effect in this cell architecture is totally eliminated. The PEO-based GPE can not only avoid the leakage and evaporation of electrolyte but also provide sufficient flexibility to maintain a relatively low interfacial resistance. In order to further improve liquid uptake of the final GPE, commercial available porous carbon paper and porous glass-fiber(GF) mat soaked with GPE slurry were stuck to the LAGP surfaces facing to cathode and anode, respectively. A simple demonstration of the GCME Li-S cell is shown in Fig. S1. As a result, the unique features of the cell configuration lead to superior cell performance with no self-discharge, high coulombic efficiency and long cycling life.

Fig. 2 and Fig. S2 shows the Scanning electron microscopy (SEM) characterizations of the GCME. The LAGP and the GPE are stuck well (marked by the circle in Fig. 2a), which is good for the transport of the Li-ion across the interface. The particles dispersed in the PEO matrix is the LAGP ceramic powder which served as inorganic filler to improve uptake of liquid electrolyte and enhance the dimensional stability of the GPE.[20, 21] The commercial carbon paper and the GF mat that consist of randomly arranged long fibers are still porous when filled with GPE, providing the possibility to further improve liquid uptake.

The ionic conductivities of the electrolyte were measured by means of impedance spectroscopy. Meanwhile, The transference numbers were evaluated by using a technique that combines both the direct current polarization and impedance spectroscopy. Total resistances of the GF mat soaked with liquid electrolyte, the GPE, the LAGP pellet and the GCME are obtained from Fig. S3 (a), (d), (e). Parameters and ionic conductivities of the GF mat and the GPE and the LAGP pellet are listed in Table S1. And the Table S2 shows the parameters

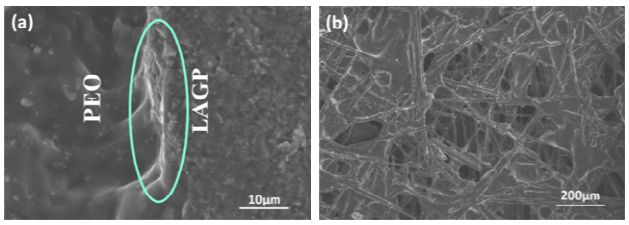

Fig. 2 (a) SEM images of the cross section of the gel-ceramic multi-layer electrolyte. (b) SEM images of porous carbon paper soaked with GPE.

and lithium ion transference number of the electrolyte calculated from Fig. S3 (b), (c). The calculated ionic conductivities of the LAGP pellet and the GCME are 1.78×10^{-4} S cm^{-1} and 1.71×10^{-4} S cm^{-1}, respectively. The GF mat soaked with liquid electrolyte and the GPE exhibit the ionic conductivities of 37.3×10^{-4} S cm^{-1} and 11.5×10^{-4} S cm^{-1} with the lithium ion transference number of 0.16 and 0.28, respectively.

Electrochemical impedance spectroscopy (EIS) measurement was conducted on the Li-S cell at fully charged state within frequency range between 0.1Hz and 1M Hz. The Nyquist plot, presented in Fig. 3a, is composed of two partially overlapped semicircles in high and medium frequency regions, and a straight slopping line at low frequency region. A possible equivalent circuit analyzed by Zview software to fit the spectrum is shown in the inset of Fig. 3a. Owing to the non-ideal behavior of the capacitor in EIS experiments, a constant phase element (CPE) is proposed here to account for it.[22, 23] R_{GCME}, which is determined by extrapolating the Nyquist plot to the real axis to an infinitely large frequency, is the ohmic resistance of the GCME. The high frequency depressed semicircle is probably derived from the interfacial contact resistance (R_{int}) between the gel electrolyte and the solid electrolyte. CPE_{int} is used here to represent its related capacitance.

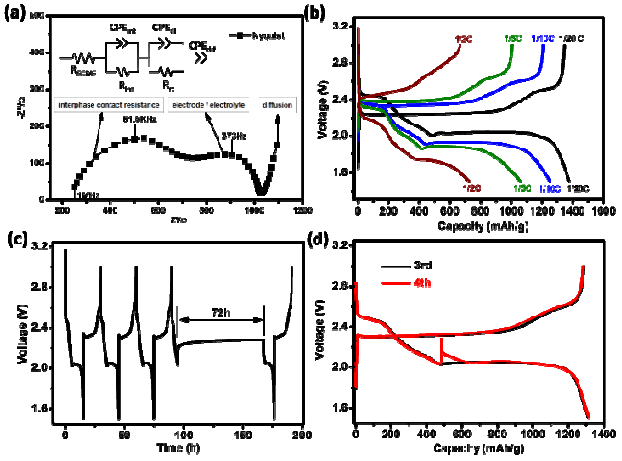

Fig.3 (a) Nyquist plot of the Li-S cell at fully charged state and inset is the proposed equivalent circuit for Li-S cell. (b) Initial discharge/charge profiles at 1/20 C, 1/10 C, 1/5 C and 1/2 C rate. Self-discharge behavior of the Li-S battery at 1/20 C: (c) The galvanostatic charge-rest-discharge curves as a function of time. (d) The corresponding galvanostatic profiles as a function of specific capacity.

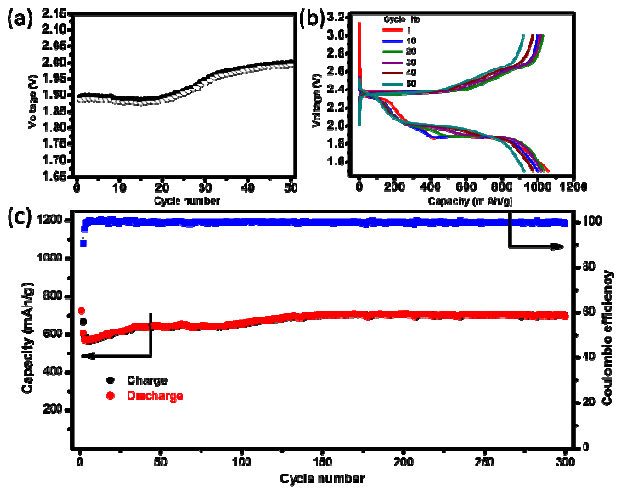

Fig. 4 (a) Medium voltage of the discharge plateau as a function of the cycle number (at 1/5 C). (b) The discharge/charge curves of the cell (at 1/5 C). (c) Long-term cycle life of the cell at 1/2 C.

R_{ct} and CPE_{dl} are the charge-transfer resistance and its relative double-layer capacitance, respectively, which correspond to the semicircle at medium frequencies. The inclined straight line at low frequency range is attributed to the CPE_{dif} that reflecting the solid-state lithium ion diffusion within the electrode.

Fig. 3b shows the initial discharge/charge profiles of the Li-S cells at different rates (1 C= 1675 mA h g^{-1}). An average open circuit voltage of about 3.2 V is observed on the as-assembled cells. There are two distinct discharge plateaus and two overlapped charge plateaus, which represent the conversion cells. There are two distinct discharge plateaus and two overlapped charge plateaus, which represent the conversion between S_8 and Li_2S via the formation of the intermediate lithium polysulfides.[1, 6] It is clear that there is a dissolution process of the intermediate polysulfides because of GPE's liquid-like Li-ion conductive mechanism.[14, 24, 25] Testing at room-temperature, specific capacities 1376, 1249, 1058 and 725 mA h g^{-1} can be achieved at C/20, C/10, C/5 and C/2 rates, respectively. The increase in polarization upon increase of current density is a result of the larger impedance of the solid electrolyte than that of the liquid electrolyte. However, no shuttle phenomenon is observed at all the rates, which is similar to our previous report.[26]

Self-discharge decreases the shelf-life of Li-S batteries and is one of the bottlenecks that greatly impedes their practical applications. Both conventional and GPE-based Li-S batteries are suffer from strong self-discharge induced by the shuttle effect.[27, 28] To assess the self-discharge of the Li-S cell, the 4th discharge was interrupted at the end of the upper plateau for 3 days (Fig. 3c) according to an advisable testing protocol.[29] After resting, discharge was resumed and the resulting galvanostatic profiles as a function of specific capacity is displayed in Fig. 3d. Compared with the 3rd cycle, the 4th cycle shows no capacity loss indicating that no self-discharge is observed. As a consequence, the GCME can effectively prevent the polysulfide anions from passing through while permit the solid-state transport of Li+ cations and avoid the unwanted side reactions.

As mentioned previously, the intermediate species formed in discharge process can be dissolved in GPE. Nevertheless, the dissolved polysulfide species are blocked by the solid electrolyte LAGP and they have no chance to migrate through and react with the lithium metal. Therefore, there is no severe capacity loss of the second cycle compared to the initial cycle. Table S2 shows the comparison of the initial capacity loss under different conditions. The GCME Li-S cells shows lager initial capacity loss at higher current density, which is possibly caused by the transport of polysulfide anions is slower than the total electrochemical reaction time. In other words, both the reversibility and utilization will be increased clearly when there is a longer time for the conversion of soluble polysulfides to the final solid discharge products. As depicted in the Fig. S3, S4, the first two discharge/charge cycle profiles of the Li-S cells at 1/20 C and 1/10 C, almost no initial capacity loss is observed. While, it is obvious that the conventional liquid electrolytes based Li-S cells exhibit severe initial capacity loss[30, 31], mainly due to the dissolution of polysulfide into the electrolyte and the subsequent shuttle reactions[32]. What's worse, the initial capacity loss of conventional Li-S cells is irreversible and the capacity fading proceeds contentiously resulting a poor cycling performance with a low coulombic efficiency.

Though initial capacity loss occurs, the GCME Li-S cell shows an increasing capacity over cycling until the initial capacity is attained to (Fig. S5). The medium voltage of the discharge plateau increases gradually from 1.9 V to 2.0 V as well , that the discharge voltage recovers its normal value from a rather high polarization, as shown in Fig. 4a. Here, medium voltage of the discharge plateau is defined as the voltage at which the discharge capacity is half of the total discharge capacity on each cycle. EIS measurement of the Li-S cell at the end of the 50th charge cycle was also carried out within frequency range between 0.1Hz and 1M Hz. As depicted in Fig. S6, compared to the Nyquist plot before cycle, the one at the 50th charge cycle shows a smaller impedance. During cycling of the Li-S cell, the soluble lithium polysulfides constrained in the GPE would probably enhance the conductivity of the GPE. Besides, GPE may help to ensure a good contact with electrodes and the solid electrolyte as observed that the interfacial resistance (represented by the high frequency depressed semicircle) shows a relatively large decrease after 50 cycles. Therefore, decrease of the resistance occurs and thus results in the rise of the lower discharge plateau (Fig. 4b). The changing discharge/charge curves indicates a different reaction mechanism from liquid electrolyte Li/S cells, as in the extreme case, the all-solid-state Li-S battery shows only one discharge plateau[33].

Long-term cycling performance of the GCME Li-S cell and hybrid liquid-solid-liquid cell are given in Fig. 4c and Fig. S7, respectively. Having an average efficiency of 100%, the cell using the hybrid liquid-solid-liquid electrolyte shows stability

over 40 cycles, following by an erratic decreasing up to 45 cycles. But then, the cell died, which largely resulted from the leakage and drying out of the liquid electrolyte. While, the Li-S cell using GCME shows a stable cycling performance after gradually recovered. With an initial specific capacity of 725 mA h g^{-1}, the cell exhibits noticeable stability with a remarkable steady-state charge and discharge up to more than 150 cycles. The specific capacity remains at 700 mA h g^{-1} after 300 cycles at C/2 rate with an excellent coulombic efficiency of 100%. The initial capacity loss and low charge–discharge efficiency of the first two cycles (91% and 97%) indicate an incomplete conversion of the discharge product. However, the solid electrolyte LAGP can eliminate the passing through of the polysulfide species and more soluble lithium polysulfides would accumulate and gradually be constrained in the GPE. It is suggested that the soluble lithium polysulfides can work as effective redox mediators to facilitate the conversion of insoluble Li_2S_2 and Li_2S.[34, 35] Additionally, GPE has the advantage of easy deformation to ensure a good contact with electrodes, recapturing of the active mass is therefore realized during the subsequent cycling.

In summary, a GCME has been synthesized and used as the separator and electrolyte for Li-S battery. The inorganic solid-state LAGP blocks the sulfur species in the cathode side and eliminates the polysulfide shuttle effect. The PEO-based GPE avoids the leakage and drying out of electrolyte and contributes to a relatively low interfacial resistance. As a result, superior cell performance with no self-discharge, high coulombic efficiency and long cycling life is demonstrated. The specific capacity of the initial cycle is 725 mA h g^{-1} and remains at 700 mA h g^{-1} after 300 cycles at C/2 rate. The unique features of the cell configuration may ultimately pave another way for construction of all-solid-state Li-S battery which is already underway and will be reported subsequently.

The authors are grateful for funding from the National Science Foundation of China (NFSC) project No. 51472261, No. 51402330 and No. 51372262; opening project of CAS Key Laboratory of Materials for Energy Conversion. Prof. B. V. R. Chowdari (Department of Physics, National University of Singapore) is greatly acknowledged for helpful discussion.

Notes and references

1. P. G. Bruce, S. A. Freunberger, L. J. Hardwick and J. M. Tarascon, *Nat Mater*, 2012, **11**, 19-29.
2. Z. Lin and C. Liang, *J. Mater. Chem. A*, 2015, **3**, 936-958.
3. J. Shim, K. A. Striebel and E. J. Cairns, *J Electrochem Soc*, 2002, **149**, A1321-A1325.
4. X. L. Ji, K. T. Lee and L. F. Nazar, *Nat Mater*, 2009, **8**, 500-506.
5. S. E. Cheon, K. S. Ko, J. H. Cho, S. W. Kim, E. Y. Chin and H. T. Kim, *J Electrochem Soc*, 2003, **150**, A800-A805.
6. A. Manthiram, Y. Fu, S. H. Chung, C. Zu and Y. S. Su, *Chem Rev*, 2014, **114**, 11751-11787.
7. G. Zheng, Y. Yang, J. J. Cha, S. S. Hong and Y. Cui, *Nano Lett*, 2011, **11**, 4462-4467.
8. Z. Lin, Z. Liu, W. Fu, N. J. Dudney and C. Liang, *Angew Chem Int Edit*, 2013, **52**, 7460-7463.
9. C. Huang, J. Xiao, Y. Shao, J. Zheng, W. D. Bennett, D. Lu, S. V. Laxmikant, M. Engelhard, L. Ji, J. Zhang, X. Li, G. L. Graff and J. Liu, *Nat Commun*, 2014, **5**, 3015.
10. X. Liang, Z. Wen, Y. Liu, M. Wu, J. Jin, H. Zhang and X. Wu, *J Power Sources*, 2011, **196**, 9839-9843.
11. N. Tachikawa, K. Yamauchi, E. Takashima, J. W. Park, K. Dokko and M. Watanabe, *Chem Commun*, 2011, **47**, 8157-8159.
12. K. Dokko, N. Tachikawa, K. Yamauchi, M. Tsuchiya, A. Yamazaki, E. Takashima, J. W. Park, K. Ueno, S. Seki, N. Serizawa and M. Watanabe, *J Electrochem Soc*, 2013, **160**, A1304-A1310.
13. Y. X. Yin, S. Xin, Y. G. Guo and L. J. Wan, *Angew Chem Int Ed Engl*, 2013, **52**, 13186-13200.
14. R. Chen, T. Zhao and F. Wu, *Chem Commun (Camb)*, 2015, **51**, 18-33.
15. J. Christensen, P. Albertus, R. S. Sanchez-Carrera, T. Lohmann, B. Kozinsky, R. Liedtke, J. Ahmed and A. Kojic, *J Electrochem Soc*, 2012, **159**, R1.
16. X. J. Wang, Y. Y. Hou, Y. S. Zhu, Y. P. Wu and R. Holze, *Sci Rep-Uk*, 2013, **3**.
17. W. B. Luo, S. L. Chou, J. Z. Wang, Y. M. Kang, Y. C. Zhai and H. K. Liu, *Chem Commun*, 2015, **51**, 8269-8272.
18. J. Y. Song, Y. Y. Wang and C. C. Wan, *J Power Sources*, 1999, **77**, 183-197.
19. K. Jeddi, M. Ghaznavi and P. Chen, *Journal of Materials Chemistry A*, 2013, **1**, 2769.
20. S. S. Zhang and D. T. Tran, *Electrochim Acta*, 2013, **114**, 296-302.
21. S. S. Zhang, *J Electrochem Soc*, 2013, **160**, A1421-A1424.
22. V. S. Kolosnitsyn, E. V. Kuzmina, E. V. Karaseva and S. E. Mochalov, *J Power Sources*, 2011, **196**, 1478-1482.
23. Z. F. Deng, Z. A. Zhang, Y. Q. Lai, J. Liu, J. Li and Y. X. Liu, *J Electrochem Soc*, 2013, **160**, A553-A558.
24. J. Jin, Z. Wen, X. Liang, Y. Cui and X. Wu, *Solid State Ionics*, 2012, **225**, 604-607.
25. Z. Jin, K. Xie, X. Hong and Z. Hu, *J Power Sources*, 2013, **242**, 478-485.
26. Q. Wang, J. Jin, X. Wu, G. Ma, J. Yang and Z. Wen, *Phys Chem Chem Phys*, 2014, **16**, 21225-21229.
27. H. S. Ryu, H. J. Ahn, K. W. Kim, J. H. Ahn, K. K. Cho and T. H. Nam, *Electrochim Acta*, 2006, **52**, 1563-1566.
28. W. T. Xu, H. J. Peng, J. Q. Huang, C. Z. Zhao, X. B. Cheng and Q. Zhang, *ChemSusChem*, 2015, **8**, 2892-2901.
29. C. J. Hart, M. Cuisinier, X. Liang, D. Kundu, A. Garsuch and L. F. Nazar, *Chem Commun (Camb)*, 2015, **51**, 2308-2311.
30. S. Wei, H. Zhang, Y. Huang, W. Wang, Y. Xia and Z. Yu, *Energ Environ Sci*, 2011, **4**, 736-740.
31. G. C. Li, W. Zhao, L. Liu and L. Chen, *Rsc Adv*, 2015, **5**, 54293-54300.
32. R. Xu, I. Belharouak, X. Zhang, R. Chamoun, C. Yu, Y. Ren, A. Nie, R. Shahbazian-Yassar, J. Lu, J. C. M. Li and K. Amine, *Acs Appl Mater Inter*, 2014, DOI: 10.1021/am504763p.
33. H. Nagata and Y. Chikusa, *J Power Sources*, 2014, **264**, 206-210.
34. Y. Yang, G. Zheng, S. Misra, J. Nelson, M. F. Toney and Y. Gui, *J Am Chem Soc*, 2012, **134**, 15387-15394.
35. L. Wang, Y. Wang and Y. Xia, *Energy Environ. Sci.*, 2015, **8**, 1551-1558.